Charged pseudoscalar and vector meson masses in strong magnetic fields in an extended NJL model

J. P. Carlomagno,[1,2] D. Gómez Dumm,[1,2] M. F. Izzo Villafañe,[3] S. Noguera,[4] and N. N. Scoccola[2,3,4]

[1]*IFLP, CONICET – Departamento de Física, Fac. de Cs. Exactas, Universidad Nacional de La Plata, C.C. 67, (1900) La Plata, Argentina*

[2]*CONICET, Rivadavia 1917, (1033) Buenos Aires, Argentina*

[3]*Physics Department, Comisión Nacional de Energía Atómica, Av. Libertador 8250, (1429) Buenos Aires, Argentina*

[4]*Departamento de Física Teórica and IFIC, Centro Mixto Universidad de Valencia-CSIC, E-46100 Burjassot (Valencia), Spain*

(Received 2 October 2022; accepted 7 November 2022; published 28 November 2022)

The mass spectrum of π^+ and ρ^+ mesons in the presence of a static uniform magnetic field $\vec{B}$ is studied within a two-flavor Nambu-Jona-Lasinio-like model. We improve previous calculations, taking into account the effect of Schwinger phases carried by quark propagators and using an expansion of meson fields in terms of the solutions of the corresponding equations of motion for nonzero B. It is shown that the meson polarization functions are diagonal in this basis. Our numerical results for the ρ^+ meson spectrum are found to disfavor the existence of a meson condensate induced by the magnetic field. In the case of the π^+ meson, π—ρ mixing effects are analyzed for the meson lowest-energy state. The predictions of the model are compared with available lattice QCD results.

DOI: 10.1103/PhysRevD.106.094035

I. INTRODUCTION

It is well known that the presence of a background magnetic field of magnitude $|B| \gtrsim 10^{19}$ G has a large impact on the physics of strongly interacting particles, giving rise to significant effects on both hadron properties and QCD phase transition features [1–3]. Such huge magnetic fields can be achieved in matter at extreme conditions, e.g., at the occurrence of the electroweak phase transition in the early Universe [4,5] or in the deep interior of compact stellar objects like magnetars [6,7]. Moreover, it has been pointed out that values of $|eB|$ ranging from m_π^2 to $15m_\pi^2$ ($|B| \sim 0.3$ to 5×10^{19} G) can be reached in noncentral collisions of relativistic heavy ions at the Relativistic Heavy Ion Collider (RHIC) and LHC experiments [8,9]. Though these large background fields are short lived, they should be strong enough to affect the hadronization process, offering the amazing possibility of recreating a highly magnetized QCD medium in the laboratory. From the theoretical point of view, the study of strong interactions in the presence of a large magnetic field includes several interesting phenomena, such as the chiral magnetic effect [10–12], which entails the generation of an electric current induced by chirality imbalance, and the so-called magnetic catalysis [13,14] and inverse magnetic catalysis [15,16], which refer to the effect of the magnetic field on the size of quark-antiquark condensates and on the restoration of chiral symmetry.

Yet another possible effect has been discussed in the past few years. It has been claimed that, for a sufficiently large external magnetic field, one could find a phase transition of the QCD vacuum into an electromagnetic superconducting state. This transition could be produced at zero temperature, driven by the emergence of quark-antiquark vector condensates that carry the quantum numbers of electrically charged ρ mesons [17,18]. The existence or not of such a superconducting (anisotropic and inhomogeneous) QCD vacuum state is presently an interesting subject of investigation and still remains as an open question [19–27].

It is clear that the study of the properties of magnetized light hadrons, in particular π and ρ mesons, comes up as a crucial task toward the understanding of the above-mentioned problems. In fact, this subject has been addressed in several works in the context of various effective schemes for QCD. These include, e.g., Nambu-Jona-Lasinio (NJL-) like models [18,25,27–42], quark-meson models [43,44], chiral perturbation theory (ChPT) [45–47], hidden local symmetry [48], path integral Hamiltonians [23,49], and QCD sum rules [50]. In addition, results for the charged π

and ρ meson spectra in the presence of background magnetic fields have been obtained from lattice QCD (LQCD) calculations [15,24,51–54].

In this article, we concentrate on the analysis of charged π^+ and ρ^+ mesons, which turn out to get mixed in the presence of an external magnetic field $\vec{B}$. Our analysis is carried out in the framework of a two-flavor NJL-like quark model [55–57]; within a similar context, the properties of magnetized neutral pseudoscalar and vector mesons have been studied in Ref. [58]. It is worth noticing that in the present case the calculations involving quark loops for nonzero B require some care due to the presence of Schwinger phases [59]. While these phases cancel out for neutral mesons, in general they do not vanish when charged mesons are considered; this has been shown explicitly in the case of charged pions in Refs. [37,40]. At the same time, instead of dealing with free charged π^+ or ρ^+ meson fields, at the zero order, one should consider the wave functions obtained as solutions of the charged meson equations of motion in the presence of a constant external magnetic field B. In fact, at the one-loop level, Schwinger phases induce a breakdown of translational invariance in quark propagators, which is compensated by the wave functions of the external π^+ or ρ^+ mesons. It is seen that the charged meson polarization functions are not diagonal for the standard plane-wave states, while they become diagonalized in the basis associated to the solutions of the corresponding equations of motion for nonzero B. In addition, it is important to care about the regularization of ultraviolet divergences, since the presence of the external magnetic field can lead to spurious results, such as unphysical oscillations of physical observables [60,61]. Here, we use the so-called magnetic field independent regularization (MFIR) scheme, [30,31,37,62], which has been shown to be free from these effects and to reduce the dependence of the results on model parameters [61]. Concerning the effective coupling constants of the model, we consider both the case in which these parameters are fixed and the case in which they depend on the external magnetic field. This last possibility, inspired by the magnetic screening of the strong coupling constant occurring for large B [63], has been previously explored in effective models [64–70] in order to reproduce the inverse magnetic catalysis effect obtained in finite-temperature LQCD calculations.

From our calculations, it is found that the energy of the ρ^+ meson fundamental state—which corresponds to a Landau level $k=-1$—does not show a large reduction for values of eB up to 1 GeV^2, in both the cases of fixed and B-dependent couplings. Hence, our approach, which improves upon previous two-flavor NJL model calculations that use a plane-wave approximation for charged meson wave functions, disfavors the existence of a charged vector meson condensate induced by the magnetic field. On the other hand, we find that for nonzero B the lowest-energy state for the π^+ state—Landau level $k=0$—gets mixed with the corresponding ρ^+ state, this mixing being quantitatively significant for eB above 0.5 GeV^2.

The paper is organized as follows. In Sec. II, we introduce the theoretical formalism used to obtain the masses of charged meson eigenstates. In particular, we obtain π^+ and ρ^+ polarization functions for the lowest Landau levels $k=-1$ and $k=0$. In Sec. III, we present and discuss our numerical results, while in Sec. IV, we provide a summary of our work, together with our main conclusions. We also include Appendixes A, B, and C to provide some formulas related with the formalism as well as some technical details of our calculations.

II. THEORETICAL FORMALISM

A. Effective Lagrangian and mean field gap equation

Let us start by considering the Euclidean action for an extended NJL two-flavor model in the presence of an electromagnetic field. We have

$$\begin{aligned} S_E = \int d^4x\{&\bar{\psi}(x)(-i\not{D}+m_c)\psi(x) \\ &- g_s[(\bar{\psi}(x)\psi(x))^2+(\bar{\psi}(x)i\gamma_5\vec{\tau}\psi(x))^2] \\ &- g_v(\bar{\psi}(x)\gamma_\mu\vec{\tau}\psi(x))^2\}, \end{aligned} \tag{1}$$

where $\psi=(ud)^T$, and m_c is the current quark mass, which is assumed to be equal for u and d quarks. The interaction between the fermions and the electromagnetic field $\mathcal{A}_\mu$ is driven by the covariant derivative

$$D_\mu = \partial_\mu - i\hat{Q}\mathcal{A}_\mu, \tag{2}$$

where $\hat{Q}=\mathrm{diag}(Q_u,Q_d)$, with $Q_u=2e/3$ and $Q_d=-e/3$, e being the proton electric charge. We consider the particular case in which one has a homogenous stationary magnetic field $\vec{B}$ orientated along the 3, or z, axis. Then, choosing the Landau gauge, we have $\mathcal{A}_\mu = Bx_1\delta_{\mu 2}$.

Since we are interested in studying meson properties, it is convenient to bosonize the fermionic theory, introducing scalar, pseudoscalar, and vector fields σ, $\vec{\pi}(x)$, and $\vec{\rho}_\mu(x)$ and integrating out the fermion fields. The bosonized Euclidean action can be written as

$$\begin{aligned} S_{\rm bos} = -\ln\det\mathcal{D} &+ \frac{1}{4g_s}\int d^4x[\sigma(x)\sigma(x)+\vec{\pi}(x)\cdot\vec{\pi}(x)] \\ &+ \frac{1}{4g_v}\int d^4x\vec{\rho}_\mu(x)\cdot\vec{\rho}_\mu(x), \end{aligned} \tag{3}$$

with

$$\mathcal{D}_{x,x'} = \delta^{(4)}(x-x')[-i\not{\partial} + m_0 + \sigma(x) + i\gamma_5\vec{\tau}\cdot\vec{\pi}(x) + \gamma_\mu\vec{\tau}\cdot\vec{\rho}_\mu(x)], \tag{4}$$

where a direct product to an identity matrix in color space is understood.

We proceed by expanding the bosonized action in powers of the fluctuations of the bosonic fields around the corresponding mean field (MF) values. We assume that the field $\sigma(x)$ has a nontrivial translational invariant MF value $\bar{\sigma}$, while the vacuum expectation values of other bosonic fields are zero. Thus, the MF action per unit volume is given by

$$\frac{S_{\rm bos}^{\rm MF}}{V^{(4)}} = \frac{\bar{\sigma}^2}{4g_s} - \frac{N_c}{V^{(4)}}\sum_{f=u,d}\int d^4x d^4x' {\rm tr}_D \ln (\mathcal{S}_{x,x'}^{{\rm MF},f})^{-1}, \tag{5}$$

where ${\rm tr}_D$ stands for the trace in Dirac space and $\mathcal{S}_{x,x'}^{{\rm MF},f} = (\mathcal{D}_{x,x'}^{{\rm MF},f})^{-1}$ is the MF quark propagator in the presence of the magnetic field. As is well known, the explicit form of the propagators can be written in different ways [2,3]. For convenience, we take the form in which $\mathcal{S}_{x,x'}^{{\rm MF},f}$ is given by a product of a phase factor and a translational invariant function, namely,

$$\mathcal{S}_{x,x'}^{{\rm MF},f} = e^{i\Phi_f(x,x')}\tilde{S}^f(x-x'), \tag{6}$$

where $\Phi_f(x,x') = Q_f B(x_1+x_1')(x_2-x_2')/2$ is the so-called Schwinger phase and $\tilde{S}^f(x-x')$ can be written as

$$\tilde{S}^f(x-x') = \int \frac{d^4p}{(2\pi)^4} e^{ip(x-x')}\tilde{S}_p^f. \tag{7}$$

Now, $\tilde{S}_p^f$ can be expressed in the Schwinger form [2,3]

$$\tilde{S}_p^f = \int_0^\infty d\tau \exp\left[-\tau\left(M^2 + p_\parallel^2 + p_\perp^2\frac{\tanh(\tau B_f)}{\tau B_f} - i\epsilon\right)\right] \times \left\{(M - p_\parallel\cdot\gamma_\parallel)[1 + is_f\gamma_1\gamma_2\tanh(\tau B_f)] - \frac{p_\perp\cdot\gamma_\perp}{\cosh^2(\tau B_f)}\right\}, \tag{8}$$

where we have used the following definitions. The perpendicular and parallel gamma matrices are collected in vectors $\gamma_\perp = (\gamma_1,\gamma_2)$ and $\gamma_\parallel = (\gamma_3,\gamma_4)$, and, similarly, we have defined $p_\perp = (p_1,p_2)$ and $p_\parallel = (p_3,p_4)$. Note that we are working in Euclidean space, where $\{\gamma_\mu,\gamma_\nu\} = -2\delta_{\mu\nu}$. Other definitions in Eq. (8) are $s_f = {\rm sign}(Q_f B)$ and $B_f = |Q_f B|$. The limit $\epsilon\to 0$ is implicitly understood.

The integral in Eq. (8) is divergent and has to be properly regularized. As stated in the Introduction, we use here the MFIR scheme: for a given unregularized quantity that depends explicitly on B, the corresponding (divergent) $B\to 0$ limit is subtracted, and then it is added in a regularized form. Thus, the quantities can be separated into a (finite) "$B=0$" part and a "magnetic" piece. Notice that, in general, the "$B=0$" part still depends implicitly on B (e.g., through the values of the dressed quark masses M); hence, it should not be confused with the value of the studied quantity at vanishing external field. To deal with the divergent "$B=0$" terms, we use here a 3D cutoff regularization scheme. In the case of the quark-antiquark condensates $\phi_f \equiv \langle\bar{\psi}_f\psi_f\rangle$, $f=u, d$, we obtain

$$\phi_f^{\rm reg} = \phi^{0,{\rm reg}} + \phi_f^{\rm mag}, \tag{9}$$

where

$$\phi^{0,{\rm reg}} = -N_c M I_1, \qquad \phi_f^{\rm mag} = -N_c M I_{1f}^{\rm mag}. \tag{10}$$

The expression of I_1 for the 3D cutoff regularization is given by Eq. (A3) of Appendix A, while the B-dependent function $I_{1f}^{\rm mag}$ reads [13,60]

$$I_{1f}^{\rm mag} = \frac{B_f}{2\pi^2}\left[\ln\Gamma(x_f) - \left(x_f - \frac{1}{2}\right)\ln x_f + x_f - \frac{\ln 2\pi}{2}\right], \tag{11}$$

where $x_f = M^2/(2B_f)$. The corresponding gap equation, obtained from $\partial S_{\rm bos}^{\rm MF}/\partial\bar{\sigma} = 0$, can be written as

$$M = m_c - 2g_s[\phi_u^{\rm reg} + \phi_d^{\rm reg}]. \tag{12}$$

B. Charged meson sector

As expected from charge conservation, it is easy to see that the contributions to the bosonic action that are quadratic in the fluctuations of charged and neutral mesons decouple from each other. We consider here the charged meson sector in the presence of the external magnetic field. A detailed analysis of the neutral sector can be found in Ref. [58]. For definiteness, we explicitly analyze the case of positively charged mesons, since the results for meson masses will not depend on the charge sign. The corresponding contribution to the quadratic action can be written as

$$S_{\rm bos}^{{\rm quad},+} = \frac{1}{2}\sum_{M,M'}\int d^4x d^4x' \delta M(x)^\dagger \mathcal{G}_{MM'}(x,x')\delta M'(x'), \tag{13}$$

where M, M' are either π^+ or ρ_μ^+, and

$$\mathcal{G}_{MM'}(x,x') = \frac{1}{2g_M}\delta_{MM'}\delta^{(4)}(x-x') + \mathcal{J}_{MM'}(x,x'), \tag{14}$$

where $\delta_{MM'}$ is an obvious generalization of the Kronecker δ, and the constants g_M are given by $g_{\pi^+} = g_s$ and $g_{\rho^+_\mu} = g_v$. The polarization functions $\mathcal{J}_{MM'}(x,x')$ read

$$\mathcal{J}_{MM'}(x,x') = e^{i[\Phi_u(x,x')+\Phi_d(x',x)]}\int \frac{d^4q}{(2\pi)^4} e^{iq(x-x')}\tilde{\mathcal{J}}_{MM'}(q), \tag{15}$$

where

$$\tilde{\mathcal{J}}_{MM'}(q) = 2N_c \int \frac{d^4p}{(2\pi)^4} \mathrm{tr}_D[\tilde{\mathcal{S}}^u_{p^+}\Gamma_{M'}\tilde{\mathcal{S}}^d_{p^-}\Gamma_M], \tag{16}$$

with $\Gamma_{\pi^+} = i\gamma_5$, $\Gamma_{\rho^+_\mu} = \gamma_\mu$ and $p^\pm = p \pm q/2$.

Contrary to the neutral meson case, here the Schwinger phases do not cancel, due to their different quark flavors. In fact, one has

$$\begin{aligned}\Phi_u(x,x') + \Phi_d(x',x) &= eB(x_1 + x'_1)(x_2 - x'_2)/2 \\ &\equiv \Phi_+(x,x'),\end{aligned} \tag{17}$$

where we have used $Q_u - Q_d = Q_{\pi^+} = Q_{\rho^+} = e$. As a consequence, the polarization functions in Eq. (15) are not translational invariant, and they do not become diagonal when transformed to the momentum basis. Instead of using the standard plane-wave decomposition, to diagonalize the polarization functions, it is necessary to expand the meson fields in terms of a set of functions $\mathbb{F}(x,\bar{q})$, associated to the solutions of the corresponding equations of motion in the presence of a constant magnetic field B. For the charged pion field, we have

$$\delta\pi^+(x) = \frac{1}{2\pi}\sum_k \int \frac{dq_2dq_3dq_4}{(2\pi)^3}\mathbb{F}(x,\bar{q})\delta\pi^+(\bar{q}), \tag{18}$$

where we have defined $\bar{q} = (k, q_2, q_3, q_4)$. Here, the index k is an integer that labels the so-called Landau modes associated to the presence of the magnetic field. The functions $\mathbb{F}(x,\bar{q})$ are given by

$$\mathbb{F}(x,\bar{q}) = N_k e^{i(q_2x_2+q_3x_3+q_4x_4)}D_k(r), \tag{19}$$

where $D_k(x)$ are the cylindrical parabolic functions with the convention $D_k(x) = 0$ for $k < 0$ (this implies that for charged pions $k = 0, 1, 2, \ldots$). We have used the definitions $N_k = (4\pi B_e)^{1/4}/\sqrt{k!}$ and $r = \sqrt{2B_e}x_1 - s\sqrt{2/B_e}q_2$, where $B_e = |Q_{\pi^+}B| = |eB|$, $s = \mathrm{sign}(Q_{\pi^+}B) = \mathrm{sign}(B)$, $Q_{\pi^+} = Q_u - Q_d = e$. It is not difficult to show that the functions in Eq. (19) are solutions of Klein-Gordon equation corresponding to a pseudoscalar meson of mass m_π in the presence of constant magnetic field when the corresponding on-shell condition $(2k+1)B_e + q_3^2 + q_4^2 + m_\pi^2 = 0$ is fulfilled.

In the case of the charged ρ mesons, we introduce a new set of functions $\mathbb{R}_{\mu\nu}(x,\bar{q})$, expanding the vector fields as

$$\delta\rho^+_\mu(x) = \frac{1}{2\pi}\sum_k \int \frac{dq_2dq_3dq_4}{(2\pi)^3}\mathbb{R}_{\mu\nu}(x,\bar{q})\delta\rho^+_\nu(\bar{q}). \tag{20}$$

The new functions are given by

$$\mathbb{R}_{\mu\nu}(x,\bar{q}) = \sum_{\ell=-1}^{1} R_\ell(x,\bar{q})\Delta^{(\ell)}_{\mu\nu}, \tag{21}$$

where

$$R_\ell(x,\bar{q}) = N_{k-s\ell}e^{i(q_2x_2+q_3x_3+q_4x_4)}D_{k-s\ell}(r). \tag{22}$$

Note that in order to have nonvanishing functions $R_\ell(x,\bar{q})$ the condition $k - s\ell \geq 0$ has to be satisfied. Given the possible values of ℓ $(0,\pm 1)$ and s (± 1), it follows that for charged rho mesons one has $k = -1, 0, 1, \ldots$. There is some freedom in the election of $\Delta^{(\ell)}$ matrices, which is compensated by the choice of the meson polarization vectors. The explicit form of the matrices used here is given in Appendix B, together with the corresponding polarization vectors $\epsilon_\nu(\bar{q},a)$, in terms of which one can write the fields $\delta\rho^+_\nu(\bar{q})$. In that Appendix, it is also shown that the functions in Eq. (21) are solutions of the Proca equation corresponding to a vector meson of mass m_ρ in the presence of constant magnetic field when the on-shell condition $(2k+1)B_e + q_3^2 + q_4^2 + m_\rho^2 = 0$ is fulfilled.

For convenience, in what follows, we introduce the shorthand notation

$$\sum\!\!\!\!\!\!\int_{\bar{q}} \equiv \frac{1}{2\pi}\sum_{k=k_{\min}}^{\infty}\int \frac{dq_2dq_3dq_4}{(2\pi)^3}, \tag{23}$$

where it is understood that $k_{\min} = -1$ (0) for rho (pion) meson fields. Hence, in the previously introduced basis, we have

$$S^{\mathrm{quad},+}_{\mathrm{bos}} = \frac{1}{2}\sum_{MM'}\sum\!\!\!\!\!\!\int_{\bar{q},\bar{q}'}\delta M(\bar{q})^\dagger \mathcal{G}_{MM'}(\bar{q},\bar{q}')\delta M'(\bar{q}'), \tag{24}$$

with

$$\mathcal{G}_{MM'}(\bar{q},\bar{q}') = \frac{1}{2g_M}\delta_{MM'}\hat{\delta}_{\bar{q}\bar{q}'} + \mathcal{J}_{MM'}(\bar{q},\bar{q}'), \tag{25}$$

where we have defined

$$\hat{\delta}_{\bar{q}\bar{q}'} \equiv (2\pi)^4\delta_{kk'}\delta(q_2 - q'_2)\delta(q_3 - q'_3)\delta(q_4 - q'_4). \tag{26}$$

In this basis, the polarization functions are given by

$$
\begin{aligned}
\mathcal{J}_{\pi^+\pi^+}(\bar{q},\bar{q}') &= \int \frac{d^4v}{(2\pi)^4}\tilde{\mathcal{J}}_{\pi^+\pi^+}(v)\int d^4x d^4x' e^{iv(x-x')}e^{i\Phi_+(x,x')}[\mathbb{F}(x,\bar{q})]^*\mathbb{F}(x',\bar{q}'),\\
\mathcal{J}_{\rho^+_\nu\rho^+_\mu}(\bar{q},\bar{q}') &= \int \frac{d^4v}{(2\pi)^4}\tilde{\mathcal{J}}_{\rho^+_\nu\rho^+_\mu}(v)\int d^4x d^4x' e^{iv(x-x')}e^{i\Phi_+(x,x')}[\mathbb{R}_{\beta\nu}(x,\bar{q})]^*\mathbb{R}_{\alpha\mu}(x',\bar{q}'),\\
\mathcal{J}_{\pi^+\rho^+_\mu}(\bar{q},\bar{q}') &= \int \frac{d^4v}{(2\pi)^4}\tilde{\mathcal{J}}_{\pi^+\rho^+_\mu}(v)\int d^4x d^4x' e^{iv(x-x')}e^{i\Phi_+(x,x')}[\mathbb{F}(x,\bar{q})]^*\mathbb{R}_{\alpha\mu}(x',\bar{q}'),\\
\mathcal{J}_{\rho^+_\mu\pi^+}(\bar{q},\bar{q}') &= \int \frac{d^4v}{(2\pi)^4}\tilde{\mathcal{J}}_{\pi^+\rho^+_\mu}(v)\int d^4x d^4x' e^{iv(x-x')}e^{i\Phi_+(x,x')}[\mathbb{R}_{\alpha\mu}(x,\bar{q})]^*\mathbb{F}(x',\bar{q}'). \qquad (27)
\end{aligned}
$$

In previous works [37,40], it has been shown that $\mathcal{J}_{\pi^+\pi^+}(\bar{q},\bar{q}')$ is diagonal in $\bar{q}$-space. Following similar procedures, it is possible to show, after some lengthy calculations, that this also holds for the other polarization functions in Eqs. (27). Namely, one can write

$$
\begin{aligned}
\mathcal{J}_{\pi^+\pi^+}(\bar{q},\bar{q}') &= \hat{\delta}_{\bar{q}\bar{q}'}J_{\pi^+\pi^+}(\bar{q}), \qquad \mathcal{J}_{\rho^+_\nu\rho^+_\mu}(\bar{q},\bar{q}') = \hat{\delta}_{\bar{q}\bar{q}'}J_{\rho^+_\nu\rho^+_\mu}(\bar{q}),\\
\mathcal{J}_{\pi^+\rho^+_\mu}(\bar{q},\bar{q}') &= \hat{\delta}_{\bar{q}\bar{q}'}J_{\pi^+\rho^+_\mu}(\bar{q}), \qquad \mathcal{J}_{\rho^+_\mu\pi^+}(\bar{q},\bar{q}') = \hat{\delta}_{\bar{q}\bar{q}'}J_{\rho^+_\mu\pi^+}(\bar{q}). \qquad (28)
\end{aligned}
$$

Moreover, we also obtain $J_{\rho^+_\mu\pi^+}(\bar{q}) \propto (0,0,q_4,-q_3)$ and, as expected, $[J_{\rho^+_\mu\pi^+}(\bar{q})]^* = J_{\pi^+\rho^+_\mu}(\bar{q})$. The importance of the presence of nonzero Schwinger phases $\Phi_+(x,x')$ can be clearly seen from Eqs. (27). If one sets $\Phi_+(x,x')$ to zero, it is possible to replace the functions $\mathbb{F}$ and $\mathbb{R}$ by usual 4-momentum plane waves, getting diagonal polarization functions $\mathcal{J}_{MM'}(q,q') \propto \delta^{(4)}(q-q')$.

We are interested in studying the meson masses, i.e., the energies of the lowest-lying meson states. These correspond to the Landau modes $k=-1$ and $k=0$. From Eqs. (28), it can be immediately seen that for the mode $k=-1$ only the polarization function $\mathcal{J}_{\rho^+_\nu\rho^+_\mu}$ is nonzero; thus, this mode corresponds to the lowest-energy charged rho meson, which does not get mixed with the pion sector. In turn, for the Landau mode $k=0$, one gets the lowest-energy charged pion, which gets coupled to the $k=0$ rho meson. In what follows, we analyze these two modes in detail.

1. $k=-1$ charged ρ meson

For $k=-1$, only $J_{\rho^+_\nu\rho^+_\mu}(\bar{q})$ is relevant. Moreover, as discussed in Appendix B, in this case, there is only one possible polarization vector available for the ρ^+ field. For $B>0$ (i.e., $s=1$), this vector is given by $\epsilon_\mu(\bar{q}_{(-1)},1) = (1,0,0,0)$, while for $B<0$ $(s=-1)$, one has $\epsilon_\mu(\bar{q}_{(-1)},1) = (0,1,0,0)$, with the notation $\bar{q}_{(k)} = (k,q_2,q_3,q_4)$. Thus, to get rid of Lorentz indices, we can calculate the function $J_{\rho^+\rho^+}(-1,\Pi^2)$, defined by

$$
J_{\rho^+\rho^+}(-1,\Pi^2) = [\epsilon_\nu(\bar{q}_{(-1)},1)]^* J_{\rho^+_\nu\rho^+_\mu}(\bar{q}_{(-1)})\epsilon_\mu(\bar{q}_{(-1)},1) \qquad (29)
$$

where Π^2 is the square of the canonical momentum [see Eq. (B14)]. For the $k=-1$ mode of a charged rho meson, one has $\Pi^2 = q_3^2+q_4^2-B_e$. The function $J_{\rho^+\rho^+}(-1,\Pi^2)$ is ultraviolet divergent and has to be regularized. As in the previous section, we consider the MFIR scheme, in which we subtract the corresponding expression in the $B\to 0$ limit and then we add it in a regularized form. In this way, we get the regularized expression

$$
J^{\text{reg}}_{\rho^+\rho^+}(-1,\Pi^2) = J^{0,\text{reg}}_{\rho}(\Pi^2) + J^{\text{mag}}_{\rho^+\rho^+}(-1,\Pi^2). \qquad (30)
$$

The function $J^{0,\text{reg}}_{\rho}(q^2)$, regularized through a 3D cutoff, is given in Eq. (A1). Notice that it has an implicit dependence on the magnetic field, through the value of the constituent quark mass M. On the other hand, the "magnetic" piece is found to be given by

$$
\begin{aligned}
J^{\text{mag}}_{\rho^+\rho^+}(-1,\Pi^2) = &-\frac{N_c}{4\pi^2}\int_0^\infty dz\int_{-1}^{1} dv\, e^{-z[M^2+(1-v^2)\Pi^2/4]}\\
&\times\left\{\frac{(1+t_u)(1+t_d)}{\alpha_+}\right.\\
&\times\left[M^2+\frac{1}{z}-\frac{1-v^2}{4}(\Pi^2+B_e)\right]e^{-z(1-v^2)B_e/4}\\
&\left.-\frac{1}{z}\left[M^2+\frac{1}{z}-\frac{1-v^2}{4}\Pi^2\right]\right\}, \qquad (31)
\end{aligned}
$$

where we have used the definitions $t_u = \tanh[(1-v)zB_u/2]$, $t_d = \tanh[(1+v)zB_d/2]$, and $\alpha_+ = t_u/B_u + t_d/B_d + B_e t_u t_d/(B_u B_d)$. Notice that, $J_{\rho^+\rho^+}(-1,\Pi^2)$ being a function of Π^2, our result is explicitly invariant under boosts in the direction of the magnetic field.

The mass of the $k=-1$ charged rho meson can be found as a solution of the equation

$$\frac{1}{2g_v} + J^{\rm reg}_{\rho^+\rho^+}(-1, -m^2_{\rho^+}) = 0, \tag{32}$$

while the associated energy will be given by $E_{\rho^+} = \sqrt{m^2_{\rho^+} - B_e}$.

By looking at the expression of the function $J^{0,{\rm reg}}_\rho(q^2)$ [see Eqs. (A1) and (A5)], one could expect that the $\mathcal{J}_{\rho^+_\nu \rho^+_\mu}$ polarization function gets an imaginary part when $m_{\rho^+} > 2M$ or, equivalently, when $E^2_{\rho^+} > 4M^2 - B_e$. In fact, in the absence of the external magnetic field, the value $m_\rho = 2M$ represents a threshold for the appearance of an absorptive part in the ρ meson propagator. This well-known feature of the NJL model is associated to the possible decay of the meson into a quark-antiquark pair and arises from the lack of confinement in this effective approach. For nonzero B, however, the actual threshold has to occur when the energy of $k = -1$ meson state satisfies $E_{\rho^+} > 2M$, i.e., for $m_{\rho^+} > m^{(-1)}_{\rm th}$, with $m^{(-1)}_{\rm th} = \sqrt{4M^2 + B_e}$. What happens in the interval $2M < m_{\rho^+} < m^{(-1)}_{\rm th}$ is that the aforementioned imaginary part cancels out with another imaginary contribution arising from the last term in the curly brackets in Eq. (31), after a proper analytic extension (notice that this term makes the integral divergent for $\Pi^2 < -4M^2$). Details of this calculation are given in Appendix C.

It is important to mention that, taking into account the ρ^+ polarization vector, it is possible to see that the spin of the ρ^+ in the $k = -1$ state satisfies $S_z = s$. In this way, the vector meson spin is shown to be aligned with the magnetic field, as expected for a positively charged meson in its lowest Landau mode.

2. k = 0 sector

Let us consider now the $k = 0$ Landau mode. In this case, there are two transverse independent polarization vectors $\epsilon_\mu(\bar{q}_{(0)}, \ell)$, $\ell = 1, 2$, whose expressions are given in Eq. (B17). Taking into account the general form $J_{\rho^+_\mu \pi^+}(\bar{q}) \propto (0, 0, q_4, -q_3)$, it is seen that in this case $[\epsilon_\mu(\bar{q}_{(0)}, 1)]^* J_{\rho^+_\mu \pi^+}(\bar{q}_{(0)}) = 0$. Thus, the charged pions only mix with one of the two possible charged rho meson polarization states. As expected, it can be shown that this state corresponds to the spin projection $S_z = 0$. We define now

$$J_{\rho^+\pi^+}(0, \Pi^2) = [\epsilon_\mu(\bar{q}_{(0)}, 2)]^* J_{\rho^+_\mu \pi^+}(\bar{q}_{(0)}),$$
$$J_{\rho^+\rho^+}(0, \Pi^2) = [\epsilon_\nu(\bar{q}_{(0)}, 2)]^* J_{\rho^+_\nu \rho^+_\mu}(\bar{q}_{(0)}) \epsilon_\mu(\bar{q}_{(0)}, 2). \tag{33}$$

Note that for $k = 0$ one has $\Pi^2 = q_3^2 + q_4^2 + B_e$, both for π^+ and ρ^+ states. Evaluating the integrals in Eq. (27), the explicit expression of the mixing piece $J_{\rho^+\pi^+}(0, \Pi^2)$ is found to be given by

$$J_{\rho^+\pi^+}(0, \Pi^2) = -i \frac{M N_c}{4\pi^2} \sqrt{\Pi^2 - B_e} \int_0^\infty dz \times \int_{-1}^1 dv \frac{t_u - t_d}{\alpha_+} e^{-z[M^2 + (1-v^2)(\Pi^2 - B_e)/4]}. \tag{34}$$

It is not difficult to see that, as expected, $J_{\rho^+\pi^+}(0, \Pi^2)$ vanishes at $B = 0$. Moreover, the integrals are finite, and thus no regularization is needed. On the other hand, both $J_{\rho^+\rho^+}(0, \Pi^2)$ and $J_{\pi^+\pi^+}(0, \Pi^2)$ turn out to be divergent. Therefore, as in the $k = -1$ case, we use the MFIR scheme to get the corresponding regularized quantities, which can be written as

$$J^{\rm reg}_{\pi^+\pi^+}(0, \Pi^2) = J^{0,{\rm reg}}_\pi(\Pi^2) + J^{\rm mag}_{\pi^+\pi^+}(0, \Pi^2),$$
$$J^{\rm reg}_{\rho^+\rho^+}(0, \Pi^2) = J^{0,{\rm reg}}_\rho(\Pi^2) + J^{\rm mag}_{\rho^+\rho^+}(0, \Pi^2). \tag{35}$$

The expressions for $J^{0,{\rm reg}}_\pi(\Pi^2)$ and $J^{0,{\rm reg}}_\rho(\Pi^2)$ are given in Appendix A. In the case of the charged pion, the expression of the magnetic piece $J^{\rm mag}_{\pi^+\pi^+}(0, \Pi^2)$ has been previously obtained in Refs. [37,40]. For the reader's convenience, we also quote it here. One has

$$J^{\rm mag}_{\pi^+\pi^+}(0, \Pi^2) = -\frac{N_c}{4\pi^2} \int_0^\infty dz \int_{-1}^1 dv \left\{ \left[\frac{1 - t_u t_d}{\alpha_+} \left(M^2 + \frac{1}{z} - \frac{1 - v^2}{4} (\Pi^2 - B_e) \right) + \frac{(1 - t_u^2)(1 - t_d^2)}{\alpha_+^2} \right] e^{-z[M^2 + (1-v^2)(\Pi^2 - B_e)/4]} - \frac{1}{z} \left[M^2 + \frac{2}{z} - \frac{1 - v^2}{4} \Pi^2 \right] e^{-z[M^2 + (1-v^2)\Pi^2/4]} \right\}. \tag{36}$$

On the other hand, for the quadratic ρ^+ term, we find

$$J^{\rm mag}_{\rho^+\rho^+}(0, \Pi^2) = -\frac{N_c}{4\pi^2} \int_0^\infty dz \int_{-1}^1 dv \left\{ \left[\frac{1 - t_u t_d}{\alpha_+} \left(M^2 - \frac{1 - v^2}{4} (\Pi^2 - B_e) \right) + \frac{(1 - t_u^2)(1 - t_d^2)}{\alpha_+^2} \right] e^{-z[M^2 + (1-v^2)(\Pi^2 - B_e)/4]} - \frac{1}{z} \left[M^2 + \frac{1}{z} - \frac{1 - v^2}{4} \Pi^2 \right] e^{-z[M^2 + (1-v^2)\Pi^2/4]} \right\}. \tag{37}$$

Once again, the polarization functions depend on Π^2; therefore, they are invariant under boosts in the direction of the magnetic field.

From the above expressions, the pole masses of the physical mesons $\tilde{\pi}^+$ and $\tilde{\rho}^+$ for the $k=0$ mode can be obtained as solutions of the equation

$$\det\begin{pmatrix} 1/(2g_s) + J^{\rm reg}_{\pi^+\pi^+}(0,-m^2) & J_{\rho^+\pi^+}(0,-m^2) \\ J_{\rho^+\pi^+}(0,-m^2)^* & 1/(2g_v) + J^{\rm reg}_{\rho^+\rho^+}(0,-m^2) \end{pmatrix} = 0, \tag{38}$$

while the associated meson energies are $E=\sqrt{m^2+B_e}$. As in the previous case, it is important to determine which is the threshold for the appearance of absorptive parts. As in the case of $J^{\rm reg}_{\rho^+\rho^+}(-1,-m^2)$, the $B=0$ terms $J^{0,{\rm reg}}_{\pi^+\pi^+}(0,-m^2)$ and $J^{0,{\rm reg}}_{\rho^+\rho^+}(0,-m^2)$ get an imaginary part when $m>2M$ [see Eqs. (A1) and (A5)]. Once again, these imaginary parts get canceled by imaginary contributions arising from the last terms in the integrands of Eqs. (36) and (37), after analytic continuation. On the other hand, by looking at the exponentials in Eqs. (34), (36), and (37), one might naively expect to have a threshold at $E=\sqrt{m^2+B_e}=2M$, above which convergence would be lost. From the physical point of view, however, this cannot be the case. To see this, let us consider a noninteracting $u\bar{d}$ pair in the presence of a magnetic field $\vec{B}=B\hat{z}$, with $B>0$. The lowest-energy state with spin projection $S_z=0$ will correspond to the configuration $u(S_z=+\frac{1}{2})\bar{d}(S_z=-\frac{1}{2})$, i.e., the u quark lying in its lowest Landau level and the d quark in its first excited Landau level. Recalling that the energy of a spin-1/2 fermion in the presence of the magnetic field quantizes as $E=\sqrt{m^2+2kQB}$, $k=0,1,\ldots$, the lowest possible energy for the noninteracting $\bar{u}d$ system will be given by $E_u+E_d=M_u+\sqrt{M_d^2+2B_e/3}$ (note that the alternative spin assignment, i.e., $u(S_z=-\frac{1}{2})\bar{d}(S_z=+\frac{1}{2})$, corresponds to a state with higher energy). In fact, what happens in our case is that the factors (t_u-t_d) and $(1-t_ut_d)$ in the integrals contribute with an additional exponential behavior that pushes the actual threshold up to $E>M+\sqrt{M^2+2B_e/3}$, or, equivalently, $m>m^{(0)}_{\rm th}$, with $m^{(0)}_{\rm th}=\sqrt{(M+\sqrt{M^2+2B_e/3})^2-B_e}$, in agreement with the physical expectation. It is worth remembering that M grows with B [58], preventing an imaginary value of the threshold mass $m^{(0)}_{\rm th}$.

Once the masses are determined, the composition of the physical meson states $|\tilde{\pi}^+\rangle$ and $|\tilde{\rho}^+\rangle$ is given by the corresponding eigenvectors that diagonalize the matrix in Eq. (38) for $m=m_{\pi^+}$ and $m=m_{\rho^+}$. Thus, the mass eigenstates can be written in terms of coefficients $c^M_{M'}$ as

$$|\tilde{\pi}^+\rangle = c^{\tilde{\pi}^+}_{\pi^+}|\pi^+\rangle + c^{\tilde{\pi}^+}_{\rho^+}|\rho^+\rangle,$$
$$|\tilde{\rho}^+\rangle = c^{\tilde{\rho}^+}_{\pi^+}|\pi^+\rangle + c^{\tilde{\rho}^+}_{\rho^+}|\rho^+\rangle. \tag{39}$$

III. NUMERICAL RESULTS

In what follows, we quote the numerical results for the quantities discussed in the previous section. We choose here the same set of model parameters as in Ref. [58], viz., $m_c=5.833$ MeV, $\Lambda=587.9$ MeV, and $g_s\Lambda^2=2.44$. For vanishing external field, this parametrization leads to an effective quark mass $M=400$ MeV and a quark-antiquark condensate $\phi^{0,{\rm reg}}=(-241\ {\rm MeV})^3$; in addition, one obtains the empirical values of the pion mass and decay constant in vacuum, namely, $m_\pi=138$ MeV and $f_\pi=92.4$ MeV. Regarding the vector couplings, we take $g_v=2.651/\Lambda^2$, which leads to $m_\rho=770$ MeV at $B=0$. The behavior of quark masses and quark-antiquark condensates as functions of B can be found in Ref. [58].

As mentioned in the Introduction, while local NJL-like models lead to magnetic catalysis at zero temperature, they fail to reproduce the so-called inverse magnetic catalysis effect observed from lattice QCD calculations for finite temperature systems. One simple way of dealing with this problem is to allow the model coupling constants to depend on the magnetic field. With this motivation, we also explore the possibility of considering magnetic field dependent four-fermion couplings. For definiteness, in the case of the B dependence of the coupling g_s, we adopt here the form proposed in Ref. [31], viz.,

$$g_s(B)=g_s\mathcal{F}(B), \tag{40}$$

where

$$\mathcal{F}(B)=\kappa_1+(1-\kappa_1)e^{-\kappa_2(eB)^2}, \tag{41}$$

with $\kappa_1=0.321$, $\kappa_2=1.31\ {\rm GeV}^{-2}$. With this assumption, it is found that the effective quark masses are less affected by the presence of the magnetic field than in the case of a constant g_s; in fact, they show a nonmonotonous behavior for increasing B, resembling the results found in Refs. [42,68]. On the other hand, the zero-temperature magnetic catalysis effect, characterized by the growth of quark-antiquark condensates with the magnetic field, is similar for both a constant coupling and for a B dependent g_s as in Eqs. (40) and (41) [31]. In the case of the vector coupling constant g_v, for consistency, we also allow for some dependence on B. Because of the common gluonic origin of g_s and g_v, we assume that both couplings

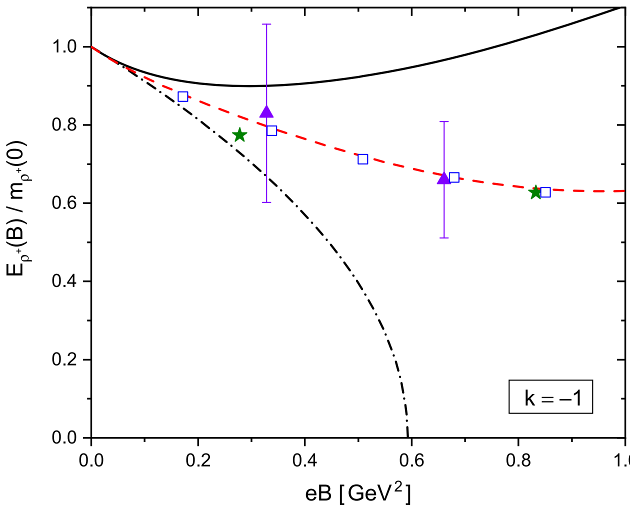

FIG. 1. Energy of the ρ^+ meson as a function of eB for the lowest Landau mode $k = -1$ and vanishing component of the momentum in the direction of $\vec{B}$. Values are normalized to the ρ^+ mass at zero external field. Solid and dashed lines correspond to fixed and B-dependent coupling constants, respectively, while the dot-dashed line corresponds to a pointlike ρ^+. For comparison, lattice QCD data quoted in Refs. [20,23,24] are also included; they are indicated by triangles, squares, and stars, respectively.

get affected in the same way by the magnetic field, and hence we take $g_v(B) = g_v \mathcal{F}(B)$.

A. $k = -1$ charged ρ meson

In Fig. 1, we show the energy of the ρ^+ meson, E_{ρ^+}, as a function of the magnetic field, for the Landau mode $k = -1$ and vanishing component of the ρ^+ momentum in the direction of $\vec{B}$. The values are normalized to the energy at $B = 0$, i.e., to the ρ meson rest mass $m_{\rho^+}(0) = E_{\rho^+}(0)$. As has been extensively discussed in the literature, if one takes the charged rho meson as a pointlike particle, the energy behaves as $E_{\rho^+}(B) = \sqrt{m_{\rho^+}^2 - eB}$, where m_{ρ^+} is a constant mass. This leads to a strong decrease with the magnetic field (dot-dashed line in Fig. 1) that reaches $E_{\rho^+}(B) = 0$ at $eB \sim 0.6$ GeV^2, triggering the appearance of a charged vector meson condensate.

As shown in Fig. 1, it is found that our results do not support the existence of this condensate. The full line in the figure corresponds to the normalized energy for the case in which the four-fermion coupling constants g_s and g_v are kept fixed. We see that, although for low values of eB the ρ^+ energy shows a decreasing behavior, at $eB \sim$ 0.2–0.3 GeV^2 the curve reaches a minimum, and for larger values of the magnetic field, the energy steadily increases. In the case in which the four-fermion couplings are taken to be dependent on B (red dashed line), the situation appears to be qualitatively similar, although the minimum is found at a larger value $eB \sim 0.9$ GeV^2. Therefore, in both situations, the model does not predict the presence of ρ^+ condensation within the considered range of values of eB. This behavior is in general consistent with the results obtained through LQCD calculations; for comparison, in Fig. 1, we include LQCD data taken from Refs. [20,23,24], indicated by triangles, squares, and stars, respectively.

It is worth mentioning that our results differ substantially from those obtained in other works in the framework of two-flavor NJL-like models [22,25], which do find ρ^+ meson condensation for $eB \sim 0.2$ to 0.6 GeV^2. In those works, the Schwinger phases are neglected, and it is assumed that charged pions and vector mesons lie in zero 3-momentum states. Here, we use, instead, an expansion of meson fields in terms of the solutions of the corresponding equations of motion for nonzero B [see Eqs. (18)–(22)], taking properly into account the presence of Schwinger phases in quark propagators. Our numerical analysis shows that this has a dramatic incidence in the numerical results, implying a qualitative change in the behavior of the ρ^+ mass for the $k = -1$ Landau mode.

B. $k = 0$ sector

In this subsection, we present and discuss the results associated with the $k = 0$ sector. As in Sec. II. B, we will concentrate on the subsystem that contains the lowest-energy pion state, i.e., the one formed by π^+ and ρ^+ states with polarization $\epsilon_\nu(\bar{q}_{(0)}, 2)$ [see Eq. (B17)], corresponding to a spin projection $S_z = 0$. As stated, the mass eigenstates denoted by $\tilde{\pi}^+$ and $\tilde{\rho}^+$ are obtained as combinations of the states π^+ and ρ^+ in Eq. (3). Here, $\tilde{\pi}^+$ and $\tilde{\rho}^+$ are expected to be the states with lower and higher energies, respectively.

The energies of the mass eigenstates as functions of the external magnetic field, normalized to the values of the corresponding masses at $B = 0$, are shown in Fig. 2. In the left panel, we display the results for the $\tilde{\pi}^+$ state; the full black line corresponds to the case in which the four-fermion couplings are kept fixed, while the red dashed line indicates the relative $\tilde{\pi}^+$ energy when g_s and g_v depend on B in the form given by Eq. (41). As a reference, the behavior of $E_{\pi^+}(B)/m_{\pi^+}(0)$ for a pointlike pion is also shown (black dot-dashed line). From the figure, it can be seen that our results for the $\tilde{\pi}^+$ state are almost independent on whether the four-fermion couplings are taken to be constant or not. Within the considered range of values of eB, in both cases, the energy shows a monotonous increasing behavior that goes slightly above the one obtained for the pointlike particle approximation. Our results for the $\tilde{\rho}^+$ energy are given in the right panel of Fig. 2, in which the same line convention is used. We see that in this case the values are somewhat more sensitive on whether the four-fermion couplings are taken to be constant or not. In both cases, the energy shows an increasing behavior, which is found to be steeper than the one obtained in the pointlike particle approximation. We also include in the graph the corresponding thresholds for the decay of the

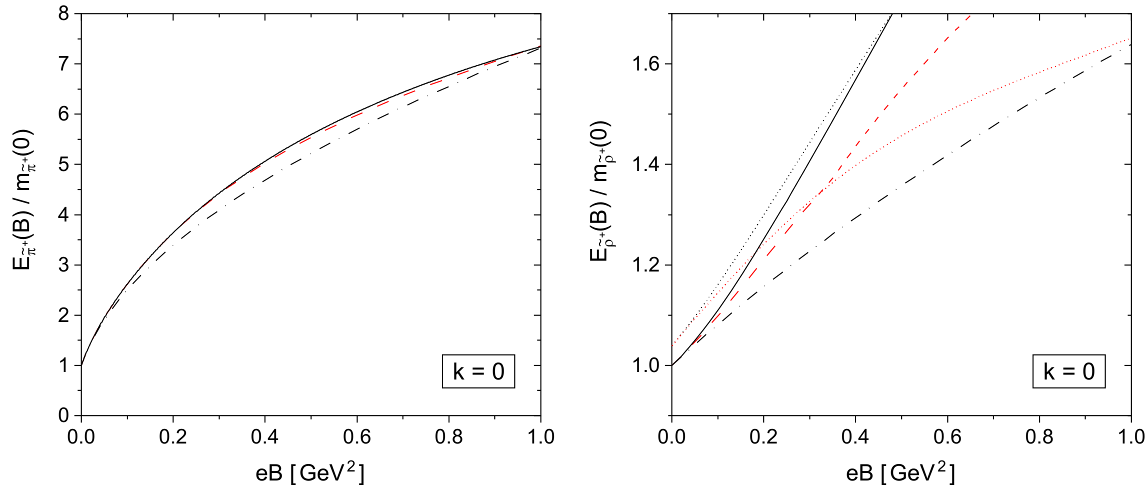

FIG. 2. Energy of the $\tilde{\pi}^+$ (left) and $\tilde{\rho}^+$ (right) mass eigenstates as functions of eB, for the Landau mode $k = 0$ and vanishing components of the momenta in the direction of $\vec{B}$. Values are normalized to the meson masses at zero external field. Solid and dashed lines correspond to fixed and B-dependent coupling constants, respectively, while dot-dashed lines correspond to the cases in which the mesons are assumed to be pointlike. In the right panel, the dotted lines indicate the thresholds for the decay of the $\tilde{\rho}^+$ meson into a $u\bar{d}$ pair. In the case of B-dependent couplings, the estimated energy beyond this threshold is shown by the red short-dashed line.

$\tilde{\rho}^+$ into a $u\bar{d}$ pair (thin short-dotted lines). If the couplings g_s and g_v are kept constant, we see that the $\tilde{\rho}^+$ energy lies below the threshold for the range plotted in the figure. On the other hand, in the case of B-dependent couplings, the corresponding threshold is reached at $eB \simeq 0.32$ GeV^2, $E_{\rho^+} \simeq 1.34 m_{\rho^+}(0)$. For larger values of the external field, the quark loop in the associated polarization function includes an absorptive piece corresponding to an unphysical decay of the $\tilde{\rho}^+$ meson into a quark-antiquark pair. As discussed in the previous section, although in this region one can still obtain results for the $\tilde{\rho}^+$ energy by means of an analytic extension of the polarization function (short-dotted red curve in the right panel of Fig. 2), these predictions have to be taken as merely indicative.

The composition of the mass eigenstates can be analyzed by looking at the coefficients $c^M_{M'}$ introduced in Eq. (39). The corresponding results for some representative values of the magnetic field are listed in Table I. They correspond to the case in which the four-fermion couplings are kept constant and are similar to those obtained in the case of B-dependent g_s and g_v. We note that, while the energies do not depend on whether B is positive or negative, the corresponding eingenvectors do; the relative signs in Table I correspond to the choice $B > 0$. As expected, for low magnetic fields (e.g., $eB = 0.05$ GeV^2), the eigenstates $\tilde{\pi}^+$ and $\tilde{\rho}^+$ are almost pure π^+ and ρ^+, respectively, while the mixing gets increased as eB grows. In the case of the $\tilde{\pi}^+$ state, we find that the ρ^+ component reaches a fraction of about $|c^{\tilde{\pi}^+}_{\rho^+}|^2 = 0.2$ (i.e., about a 20%) at $eB = 1$ GeV^2. For the $\tilde{\rho}^+$ state, the admixture grows faster with eB, both π^+ and ρ^+ components having approximately equal weight for $eB = 0.5$ GeV^2 (i.e., close to the threshold for quark-antiquark production; see the short-dotted black curve in the right panel of Fig. 2).

TABLE I. Composition of the $k = 0$, $S_z = 0$ charged meson mass eigenstates for some selected values of eB. Relative signs correspond to the choice $B > 0$.

State	eB(GeV^2)	$c^{\tilde{\pi}^+}_{\pi^+}$	$c^{\tilde{\pi}^+}_{\rho^+}$
$\tilde{\pi}^+$	0.05	0.999	0.013
	0.5	0.960	0.281
	1.0	0.892	0.453
State	eB (GeV^2)	$c^{\tilde{\rho}^+}_{\pi^+}$	$c^{\tilde{\rho}^+}_{\rho^+}$
$\tilde{\rho}^+$	0.05	−0.156	0.988
	0.5	−0.702	0.713

Let us now analyze the impact of the pseudoscalar-vector mixing on the energies of the $\tilde{\pi}^+$ and $\tilde{\rho}^+$ states. In Fig. 3, we show the dependence of these energies on the magnetic field, considering both the case in which the mixing is taken into account (full black lines) and the situation in which the off-diagonal polarization function $J_{\rho^+\pi^+}$ in Eq. (34) is set to zero (dashed green lines). The values correspond to the case in which the four-fermion couplings are kept constant; similar results are found for B-dependent couplings. It is seen that, as expected, the mixing leads to a "repulsion" between the $\tilde{\pi}^+$ and $\tilde{\rho}^+$ states: the energy of $\tilde{\pi}^+$ is reduced, while that of the $\tilde{\rho}^+$ becomes enhanced. The repulsion gets larger as eB increases, reaching an effect of about 20% for the $\tilde{\pi}^+$ energy at $eB = 1$ GeV^2.

Next, in Fig. 4, we compare our results for $\tilde{\pi}^+$ energies with those obtained in lattice QCD analyses. The curves show the values of squared E_{π^+} energies with respect to

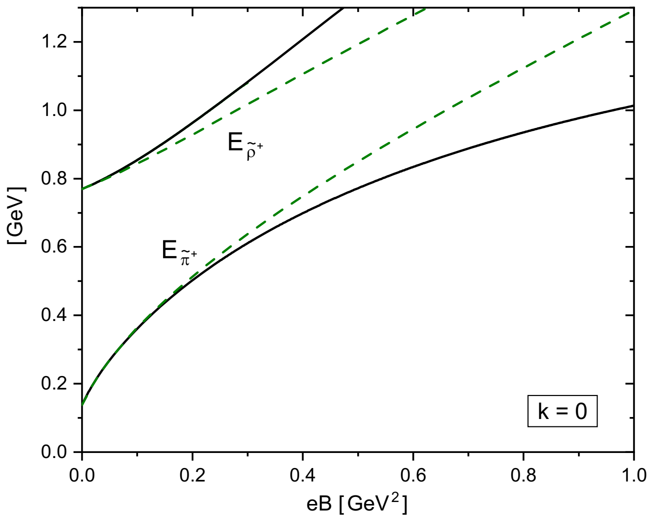

FIG. 3. Energies of the $\tilde{\pi}^+$ and $\tilde{\rho}^+$ mass eigenstates as functions of eB, for the Landau mode $k = 0$ and vanishing components of the momenta in the direction of $\vec{B}$. Solid and dashed lines correspond to the calculations with and without the inclusion of the $\rho^+ - \pi^+$ mixing terms, respectively.

$B = 0$ squared masses, considering both our numerical calculations with (full black line) and without (dashed green line) pseudoscalar-vector meson mixing. As in Fig. 3, the plots correspond to the case in which g_s and g_v do not depend on B. Open blue squares correspond to lattice QCD results from Ref. [23], obtained using quenched Wilson fermions and $m_\pi(B = 0) = 395$ MeV, while full brown

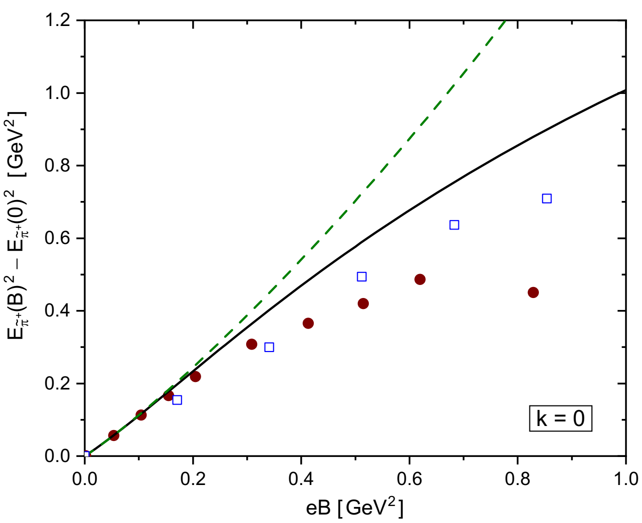

FIG. 4. Squared energy of the $\tilde{\pi}^+$ mass eigenstate for the Landau mode $k = 0$ and vanishing component of the momentum in the direction of $\vec{B}$. Values are given with respect to the squared mass for vanishing external field. Solid and dashed lines correspond to the calculations with and without the inclusion of the $\rho^+ - \pi^+$ mixing terms, respectively. For comparison, lattice QCD data from Ref. [23] (open blue squares) and Ref. [54] (full brown circles) are also shown.

circles correspond to the simulations reported in Ref. [54], which were performed using a highly improved staggered quark action with $m_\pi(B = 0) = 220$ MeV. We observe that the incorporation of the $\pi^+ - \rho^+$ mixing improves the agreement between NJL model and LQCD results. However, it is seen that the effect is not strong enough to account for the nonmonotonous behavior shown by the data from Ref. [54] for large values of the magnetic field. Regarding the $\tilde{\rho}^+$ state, lattice results show some variation depending on the lattice spacing and the simulation method (see, e.g., Refs. [23,24,53]). In any case, it is found that in general the $\tilde{\rho}^+$ energy shows an increasing behavior with the magnetic field, in qualitative agreement with our results in the right panel of Fig. 2. The results are found to be similar for the case of B-dependent coupling constants.

Finally, to see how the phase factor affects the $\tilde{\pi}^+$ mass, it is interesting to compare our results with those quoted in Ref. [36], in which Schwinger phases were not taken into account. For a proper comparison we restrict—as done in that work—to the case in which $\pi^+ - \rho^+$ mixing effects are not included. The results in Ref. [36] show that the mass of $\tilde{\pi}^+$ has a faster increase with the magnetic field than in our approach. For example, at $eB = 1$ GeV^2, they get $E_\pi(B)/m_\pi(0) \approx 15$, to be compared with our value $E_\pi(B)/m_\pi(0) \approx 9$. Notice that this steeper behavior implies a larger departure from LQCD results.

IV. SUMMARY AND CONCLUSIONS

In this work, we have studied the mass spectrum of π^+ and ρ^+ mesons in the presence of an external uniform magnetic field $\vec{B}$. This has been done in the framework of a two-flavor NJL-like model that includes scalar, pseudoscalar, and vector four-fermion couplings. Because of the presence of Schwinger phases, which induce the breakdown of translational invariance in quark propagators, it is seen that charged meson polarization functions do not become diagonal in the momentum basis. Here, we have performed the calculation of π^+ and ρ^+ polarization functions using an expansion of the meson fields in terms of the solutions of the equations of motion in the presence of the magnetic field. To account for the ultraviolet divergences that usually arise in NJL-like models, we have considered a magnetic field independent regularization, which has been shown to reduce the dependence of the results on the model parameters. Concerning the effective coupling constants of the model, we have considered both the case in which these parameters are fixed and the one in which they depend on the external magnetic field.

In the case of the ρ^+ meson, our numerical calculations show that its lowest-energy state, which corresponds to a Landau level $k = -1$, lies above ~500 MeV for values of eB up to 1 GeV^2, both for the cases of fixed and B-dependent couplings. In this way, our results—which improve upon previous two-flavor NJL model calculations that neglect Schwinger phases and use a plane-wave approximation for charged meson wave functions—are not compatible with the existence of a charged vector meson condensate induced by the magnetic field. It is found that the ρ^+ state has a lower energy in the case of B-dependent couplings, which leads to a better agreement with the results from lattice QCD calculations.

Concerning the π^+ meson, it is seen that its lowest-energy state, which corresponds to the Landau level $k = 0$, gets mixed with the corresponding ρ^+ state for nonzero B. Our numerical results, both for the cases of constant and B-dependent couplings, show that the inclusion of nonzero Schwinger phases and mixing effects soften the increase of the energy $E_{\tilde{\pi}^+}$ as a function of the magnetic field, leading to energy values that lie slightly above those obtained for a pointlike particle. This softening effect is found to be favored by a comparison with lattice QCD results.

For simplicity, in the present work, we have not taken into account axial-vector interactions. We expect to address their effect in a future publication.

ACKNOWLEDGMENTS

N. N. S. would like to thank the Department of Theoretical Physics of the University of Valencia, where part of this work has been carried out, for their hospitality within the Visiting Professor program of the University of Valencia. This work has been partially funded by CONICET (Argentina) under Grant No. PIP17-700; by ANPCyT (Argentina) under Grants No. PICT17-03-0571, No. PICT19-0792, and No. PICT20-01847; by the National University of La Plata (Argentina) Project No. X824; by Ministerio de Ciencia e Innovación and Agencia Estatal de Investigación (Spain) and European Regional Development Fund Grant No. PID2019–105439GB-C21; by EU Horizon 2020 Grant No. 824093 (STRONG-2020); and by Conselleria de Innovación, Universidades, Ciencia y Sociedad Digital, Generalitat Valenciana GVA PROMETEO/2021/083.

APPENDIX A: POLARIZATION FUNCTIONS AT $B = 0$

In this Appendix, we provide the expressions of the regularized polarization functions $J_\pi^{0,\text{reg}}(q^2)$ and $J_\rho^{0,\text{reg}}(q^2)$, obtained in the limit $B = 0$ [71]. Notice that the mixing polarization functions $J_{\rho_\mu^+\pi^+}(\bar{q})$ and $J_{\pi^+\rho_\mu^+}(\bar{q})$ are zero in this limit. One has

$$J_\pi^{0,\text{reg}}(q^2) = -2N_c[I_1^{\text{reg}} + q^2 I_2^{\text{reg}}(q^2)],$$
$$J_\rho^{0,\text{reg}}(q^2) = \frac{4N_c}{3}[(2M^2 - q^2)I_2^{\text{reg}}(q^2) - 2M^2 I_2^{\text{reg}}(0)], \tag{A1}$$

where I_1^{reg} and $I_2^{\text{reg}}(q^2)$ are regularized expressions of the integrals

$$I_1 = 4\int \frac{d^4p}{(2\pi)^4}\frac{1}{p^2+M^2},$$
$$I_2(q^2) = -2\int \frac{d^4p}{(2\pi)^4}\frac{1}{[(p+q/2)^2+M^2][(p-q/2)^2+M^2]}. \tag{A2}$$

Within the 3D-cutoff regularization scheme used in this work, the first of these integrals is given by [56,71]

$$I_1^{\text{reg}} = \frac{1}{2\pi^2}\left[\Lambda^2 r_\Lambda + M^2 \ln\left(\frac{M}{\Lambda(1+r_\Lambda)}\right)\right], \tag{A3}$$

where we have defined $r_\Lambda = \sqrt{1 + M^2/\Lambda^2}$. In the case of $I_2(q^2)$, we note that in order to determine the meson masses the external momentum q has to be extended to the region $q^2 < 0$. Hence, we find it convenient to write $q^2 = -m^2$, where m is a positive real number. Then, within the 3D-cutoff regularization scheme, the regularized real part of $I_2(-m^2)$ can be written as [71]

$$\text{Re}[I_2^{\text{reg}}(-m^2)] = -\frac{1}{4\pi^2}\left[\text{arcsinh}\left(\frac{\Lambda}{M}\right) - F(m^2)\right], \tag{A4}$$

where

$$F(m^2) = \begin{cases} \sqrt{4M^2/m^2 - 1}\ \text{arctan}\left(\frac{1}{r_\Lambda\sqrt{4M^2/m^2-1}}\right) & \text{if}\ \ m^2 < 4M^2 \\ \sqrt{1 - 4M^2/m^2}\ \text{arccoth}\left(\frac{1}{r_\Lambda\sqrt{1-4M^2/m^2}}\right) & \text{if}\ \ 4M^2 < m^2 < 4(M^2+\Lambda^2) \\ \sqrt{1 - 4M^2/m^2}\ \text{arctanh}\left(\frac{1}{r_\Lambda\sqrt{1-4M^2/m^2}}\right) & \text{if}\ \ m^2 > 4(M^2+\Lambda^2) \end{cases}.$$

For the regularized imaginary part, we get

$$\text{Im}[I_2^{\text{reg}}(-m^2)] = \begin{cases} -\frac{1}{8\pi}\sqrt{1-4M^2/m^2} & \text{if}\ \ 4M^2 < m^2 < 4(M^2+\Lambda^2) \\ 0 & \text{otherwise} \end{cases}. \tag{A5}$$

APPENDIX B: VECTOR MESONS IN AN EXTERNAL MAGNETIC FIELD

In this Appendix, we show that the functions introduced in Eq. (20) correspond to solutions of the equations of motion of a charged vector meson in the presence of a constant magnetic field, provided the associated dispersion relation

$$E^2 = -q_4^2 = m^2 + (2k+1)B_Q + q_3^2 \tag{B1}$$

is satisfied.

We start from the equation of motion for a spin 1 field given in Ref. [72]. In Euclidean space, one has

$$[(D_\alpha D_\alpha - m^2)\delta_{\mu\nu} + 2iQF_{\mu\nu}]V_\nu(x) = 0, \tag{B2}$$

which has to be supplemented by the transversality condition

$$D_\mu V_\mu(x) = 0. \tag{B3}$$

In these equations, Q stands for the electric charge of the vector field $V_\mu(x)$, the covariant derivative D_α is given by $D_\alpha = \partial_\alpha - iQ\mathcal{A}_\alpha$, and $F_{\mu\nu} = \partial_\mu \mathcal{A}_\nu - \partial_\nu \mathcal{A}_\mu$. For the particular case of constant magnetic field along the z axis, using the Landau gauge, one has $\mathcal{A}_\mu = Bx_1\delta_{\mu 2}$, and Eq. (B2) reduces to

$$(\mathbb{D}_{\mu\nu} - m^2\delta_{\mu\nu})V_\nu(x) = 0, \tag{B4}$$

where $\mathbb{D}$ is a 4×4 matrix given by

$$\mathbb{D} = \left[(\nabla_1^2 + (\nabla_2 - isB_Q x_1)^2 + \nabla_3^2 + \nabla_4^2)\begin{pmatrix} \mathbb{1} & 0 \\ 0 & \mathbb{1} \end{pmatrix} + 2sB_Q \begin{pmatrix} \sigma_2 & 0 \\ 0 & 0 \end{pmatrix}\right], \tag{B5}$$

where $s = \mathrm{sign}(QB)$, $B_Q = |QB|$ and σ_2 is a Pauli matrix. Note that each entry in the matrices appearing in this equation should be understood as a 2×2 matrix, with $\mathbb{1} = \mathrm{diag}(1,1)$.

Next, let us consider a function of the form introduced in Eq. (20), namely,

$$V_\mu(x) = \mathbb{R}_{\mu\nu}(x,\bar{q})e_\nu(\bar{q}), \tag{B6}$$

with $\bar{q} = (k, q_2, q_3, q_4)$. As in the main text, the functions $\mathbb{R}_{\mu\nu}(x,\bar{q})$ are defined as

$$\mathbb{R}_{\mu\nu}(x,\bar{q}) = \sum_{\ell=-1}^{1} R_\ell(x,\bar{q})\Delta_{\mu\nu}^{(\ell)}, \tag{B7}$$

where

$$R_\ell(x,\bar{q}) = N_{k-s\ell}e^{i(q_2x_2+q_3x_3+q_4x_4)}D_{k-s\ell}(r). \tag{B8}$$

Here, $D_n(x)$ are the cylindrical parabolic functions, with the convention $D_n(x) = 0$ if $n < 0$, and we have used the definitions $N_n = (4\pi B_Q)^{1/4}/\sqrt{n!}$ and $r = s\sqrt{2/B_Q}(sB_Q x_1 - q_2)$. The 4×4 matrices $\Delta^{(\ell)}$, $\ell = -1$, 0, 1 are given by

$$\Delta^{(1)} = \frac{1}{\sqrt{2}}\begin{pmatrix} 0 & 1 & 0 & 0 \\ 0 & -i & 0 & 0 \\ 0 & 0 & 0 & 0 \\ 0 & 0 & 0 & 0 \end{pmatrix}, \quad \Delta^{(0)} = \begin{pmatrix} 0 & 0 & 0 & 0 \\ 0 & 0 & 0 & 0 \\ 0 & 0 & 1 & 0 \\ 0 & 0 & 0 & 1 \end{pmatrix},$$
$$\Delta^{(-1)} = \frac{1}{\sqrt{2}}\begin{pmatrix} 1 & 0 & 0 & 0 \\ i & 0 & 0 & 0 \\ 0 & 0 & 0 & 0 \\ 0 & 0 & 0 & 0 \end{pmatrix}. \tag{B9}$$

The election of these matrices is not unique; the above form has been chosen taking into account that the operator in Eq. (B5) is diagonal in the (3,4) subspace, while it leads to a mixing between components 1 and 2. Note that, in order to have nonvanishing solutions, we must have $k - s\ell \geq 0$. Given the possible values of ℓ ($= 0, \pm 1$) and s ($= \pm 1$), this implies that $k \geq -1$.

Using the explicit form of $\mathbb{R}_{\mu\nu}(x,\bar{q})$, it is not difficult to prove the relation

$$\mathbb{D}_{\alpha\beta}\mathbb{R}_{\beta\gamma}(x,\bar{q}) = -[(2k+1)B_Q + q_3^2 + q_4^2]\mathbb{R}_{\alpha\gamma}(x,\bar{q}). \tag{B10}$$

In this way, it follows that the functions $V_\mu(x)$ in Eq. (B6) are solutions of Eq. (B2), provided Eq. (B1) is satisfied. In fact, these functions are equivalent to those introduced by Ritus [73] for the case of spin 1/2 fermions.

To determine the set of vectors $e_\nu(\bar{q})$ that satisfy the transversality condition in Eq. (B3), it is convenient to consider the identity

$$D_\mu \mathbb{R}_{\mu\nu}(x,\bar{q}) = iR_0(x,\bar{q})[\Pi_\nu(\bar{q})]^*, \tag{B11}$$

where

$$\Pi_\nu(\bar{q}) = (is\sqrt{B_Q k_-}, -is\sqrt{B_Q k_+}, q_3, q_4), \tag{B12}$$

with $k_\pm = k + (1 \mp s)/2$. From Eqs. (B6) and (B11), the transversality condition can be expressed as

$$[\Pi_\nu(\bar{q})]^* e_\nu(\bar{q}) = 0. \tag{B13}$$

Note that $\Pi_\nu(\bar{q})$ plays here the same role as the 4-momentum in the $B = 0$ case. In fact, it is easy to see that

$$\Pi^2 \equiv [\Pi_\nu(\bar{q})]^*\Pi_\nu(\bar{q}) = (2k+1)B_Q + q_3^2 + q_4^2, \tag{B14}$$

which implies that the condition in Eq. (B1) leads to $\Pi^2 = -m^2$.

We denote by $\epsilon_\nu(\bar{q}, a)$ each of the independent normalized solutions of Eq. (B13). They correspond to the different possible polarization vectors of the spin-1 field. For $k \geq 1$, one can find three independent solutions. In that case, using the notation $\bar{q}_{(k)} = (k, q_2, q_3, q_4)$, and taking for definiteness $s = +1$, we can choose a basis formed by the vectors

$$\epsilon_\nu(\bar{q}_{(k)}, 1) = \frac{(q_\parallel^2, 0, iq_3\sqrt{(k+1)B_Q}, iq_4\sqrt{(k+1)B_Q})}{\sqrt{q_\parallel^2[(k+1)B_Q + q_\parallel^2]}},$$

$$\epsilon_\nu(\bar{q}_{(k)}, 2) = \frac{(0, 0, iq_4, -iq_3)}{\sqrt{-q_\parallel^2}},$$

$$\epsilon_\nu(\bar{q}_{(k)}, 3) = \frac{(-B_Q\sqrt{k(k+1)}, -[(k+1)B_Q + q_\parallel^2], iq_3\sqrt{kB_Q}, iq_4\sqrt{kB_Q})}{\sqrt{\Pi^2[(k+1)B_Q + q_\parallel^2]}}, \tag{B15}$$

where $q_\parallel^2 = q_3^2 + q_4^2$. For $s = -1$, the corresponding results can be obtained by exchange of the first two components of these vectors.

Because of the restrictions imposed by the condition $k - s\ell \geq 0$, the situations for $k = -1$ and $k = 0$ have to be considered separately. In the case $k = -1$, from Eqs. (B7) and (B8), it is seen that only one independent solution of the form given by Eq. (B6) can be constructed. The associated polarization vector is

$$\epsilon_\nu(\bar{q}_{(-1)}, 1) = (1, 0, 0, 0) \tag{B16}$$

for $s = 1$, and $\epsilon_\nu(\bar{q}_{(-1)}, 1) = (0, 1, 0, 0)$ for $s = -1$. On the other hand, for $k = 0$, two independent transverse solutions can be constructed. In this case, a suitable choice for the polarization vectors is

$$\epsilon_\nu(\bar{q}_{(0)}, 1) = (\delta_{1s}q_\parallel^2, \delta_{-1s}q_\parallel^2, iq_3\sqrt{B_Q}, iq_4\sqrt{B_Q})/\sqrt{q_\parallel^2(q_\parallel^2 + B_Q)},$$

$$\epsilon_\nu(\bar{q}_{(0)}, 2) = (0, 0, iq_4, -iq_3)/\sqrt{-q_\parallel^2}. \tag{B17}$$

Replacing the polarization vectors (B15) in Eq. (B6), and using the on-shell condition Eq. (B1), one recovers the known solutions for a vector boson in a constant magnetic field (see, e.g., Ref. [74]) written in Euclidean space.

Finally, note that for $k \geq 0$ an extra "longitudinal" polarization vector $\epsilon_\nu(\bar{q}_{(k)}, 4)$ can be defined as

$$\epsilon_\nu(\bar{q}_{(k)}, 4) = \Pi_\nu(\bar{q})/\sqrt{-\Pi^2}. \tag{B18}$$

In the case $k = -1$, the relation in Eq. (B3) is always satisfied. Therefore, no longitudinal polarization can be constructed.

APPENDIX C: ANALYTIC CONTINUATION OF POLARIZATION FUNCTIONS

In this Appendix, we discuss how to evaluate the magnetic contributions to the polarization functions for energies beyond the threshold of $2M$. The integrals to be analyzed are those given by Eqs. (31), (34), (36), and (37).

Let us start by considering the integral in Eq. (31), which corresponds to the ρ^+ polarization function for the $k = -1$ Landau mode. It is convenient to separate this integral into ultraviolet and infrared pieces, namely,

$$J^{\rm mag}_{\rho^+\rho^+}(-1, -m^2) = J^{\rm uv}_{\rho^+\rho^+}(-1, -m^2) + J^{(B){\rm ir}}_{\rho^+\rho^+}(-1, -m^2) + J^{(0){\rm ir}}_{\rho^+\rho^+}(-m^2), \tag{C1}$$

where

$$J^{\rm uv}_{\rho^+\rho^+}(-1, -m^2) = -\frac{N_c}{4\pi^2}\int_{-1}^{1} dv \int_0^{4/m^2} dz e^{-z[M^2-(1-v^2)m^2/4]} \times \left\{\frac{(1+t_u)(1+t_d)}{\alpha_+}\left[M^2 + \frac{1}{z} + \frac{1-v^2}{4}(m^2 - B_e)\right] e^{-z(1-v^2)B_e/4} - \frac{1}{z}\left[M^2 + \frac{1}{z} + \frac{1-v^2}{4}m^2\right]\right\},$$

$$J^{(B){\rm ir}}_{\rho^+\rho^+}(-1, -m^2) = -\frac{N_c}{4\pi^2}\int_{-1}^{1} dv \int_{4/m^2}^{\infty} dz e^{-z[M^2-(1-v^2)(m^2-B_e)/4]}\frac{(1+t_u)(1+t_d)}{\alpha_+}\left[M^2 + \frac{1}{z} + \frac{1-v^2}{4}(m^2 - B_e)\right],$$

$$J^{(0){\rm ir}}_{\rho^+\rho^+}(-m^2) = \frac{N_c}{4\pi^2}\int_{-1}^{1} dv \int_{4/m^2}^{\infty} \frac{dz}{z} e^{-z[M^2-(1-v^2)m^2/4]}\left(M^2 + \frac{1}{z} + \frac{1-v^2}{4}m^2\right). \tag{C2}$$

It is easy to see that the threshold for the appearance of absorptive parts for $J^{\rm uv}_{\rho^+\rho^+}(-1,-m^2)$ and $J^{(B){\rm ir}}_{\rho^+\rho^+}(-1,-m^2)$ is given by $m_{\rm th}^{(-1)} = \sqrt{4M^2+B_e}$. On the other hand, the $J^{(0){\rm ir}}_{\rho^+\rho^+}(-1,-m^2)$ is divergent for $m^2 \geq 4M^2$. To go beyond this limit, one can perform an analytic continuation. It can be seen that after integration over z one gets

$$J^{(0){\rm ir}}_{\rho^+\rho^+}(-m^2) = \frac{N_c m^2}{8\pi^2}\left[\frac{\sqrt{\pi}}{2}{\rm erf}(1)\exp(\beta^2) + \int_{-1}^{1} dv(1-v^2)E_1(v^2-\beta^2)\right], \tag{C3}$$

where $\beta^2 = 1–4M^2/m^2$, ${\rm erf}(x)$ is the error function, and $E_1(x)$ is the exponential integral, which can be written as

$$E_1(x) = -\gamma - \ln x + E_{\rm in}(x), \tag{C4}$$

with $E_{\rm in}(x) = \sum_{k=1}^{\infty}(-1)^{k+1}x^k/(k!k)$. For m^2 larger than $4M^2$ (i.e., $\beta^2 > 0$), the logarithm in Eq. (C4) can be extended as $\ln(x - i\epsilon) = \ln|x| - i\pi$ for negative values of x. This leads to a finite expression for $J^{(0){\rm ir}}_{\rho^+\rho^+}(-m^2)$ that includes an imaginary part

$$\begin{aligned}{\rm Im}[J^{(0){\rm ir}}_{\rho^+\rho^+}(-m^2)] &= \frac{N_c m^2}{8\pi}\int_{-\beta}^{\beta} dv(1-v^2) \\ &= \frac{N_c}{6\pi}\beta(m^2+2M^2),\end{aligned} \tag{C5}$$

which cancels exactly with the imaginary part arising from the regularized $B = 0$ piece of the polarization function $J^{0,{\rm reg}}_{\rho}(-m^2)$; see Eqs. (A1) and (A5). Thus, it is seen that the threshold $m^2 = 4M^2$ is only apparent, the actual threshold for quark-antiquark pair production in this case being located at $m_{\rm th}^{(-1)}$.

The situation is similar in the case of the $k = 0$ Landau mode. However, the corresponding quark-antiquark production threshold $m_{\rm th}^{(0)}$ is lower than $m_{\rm th}^{(-1)}$; hence, it is interesting to obtain the expressions for the analytic continuation of the polarization functions even beyond this limit. Let us consider the function $J^{\rm mag}_{\rho^+\rho^+}(0,-m^2)$, given by Eq. (37). It is convenient to separate it into four terms, namely,

$$J^{\rm mag}_{\rho^+\rho^+}(0,-m^2) = J^{\rm uv}_{\rho^+\rho^+}(0,-m^2) + J^{(B1){\rm ir}}_{\rho^+\rho^+}(0,-m^2) + J^{(B2){\rm ir}}_{\rho^+\rho^+}(0,-m^2) + J^{(0){\rm ir}}_{\rho^+\rho^+}(-m^2), \tag{C6}$$

where

$$\begin{aligned}
J^{\rm uv}_{\rho^+\rho^+}(0,-m^2) &= -\frac{N_c}{4\pi^2}\int_{-1}^{1} dv\left\{\int_0^{4/(m^2+B_e)} dz\, e^{-z[M^2-(1-v^2)(m^2+B_e)/4]}\right.\\
&\quad\times\left[\frac{(1-t_ut_d)}{\alpha_+}\left(M^2+\frac{1-v^2}{4}(m^2+B_e)\right)+\frac{(1-t_u^2)(1-t_d^2)}{\alpha_+^2}\right]\\
&\quad\left.-\int_0^{4/m^2}\frac{dz}{z}e^{-z[M^2-(1-v^2)m^2/4]}\left(M^2+\frac{1}{z}+\frac{1-v^2}{4}m^2\right)\right\},\\
J^{(B1){\rm ir}}_{\rho^+\rho^+}(0,-m^2) &= -\frac{N_c}{4\pi^2}\int_{-1}^{1} dv\int_{4/(m^2+B_e)}^{\infty} dz\, e^{-z[M^2-(1-v^2)(m^2+B_e)/4]}\\
&\quad\times\left[\left(\frac{(1-t_ut_d)}{\alpha_+}-\frac{2B_e}{9}e^{-z(1+v)B_e/3}\right)\left(M^2+\frac{1-v^2}{4}(m^2+B_e)\right)+\frac{(1-t_u^2)(1-t_d^2)}{\alpha_+^2}\right],\\
J^{(B2){\rm ir}}_{\rho^+\rho^+}(0,-m^2) &= -\frac{N_cB_e}{18\pi^2}\int_{-1}^{1} dv\int_{4/(m^2+B_e)}^{\infty} dz\, e^{-z[M^2-(1-v^2)(m^2+B_e)/4+(1+v)B_e/3]}\left[M^2+\frac{1-v^2}{4}(m^2+B_e)\right],
\end{aligned} \tag{C7}$$

while $J^{(0){\rm ir}}_{\rho^+\rho^+}(-m^2)$ is the same function analyzed in the $k = -1$ case (and the cancellation of its imaginary part proceeds in the same way as discussed above). After some analysis, it can be shown that the integrals in $J^{(B2){\rm ir}}_{\rho^+\rho^+}(0,-m^2)$ are convergent for $m^2 < m_{\rm th}^{(0)2} = (M + \sqrt{M^2+2B_e/3})^2 - B_e$, whereas for $J^{(B1){\rm ir}}_{\rho^+\rho^+}(0,-m^2)$, the region of convergence extends up to $m_{\rm th}^{(0)\prime 2} = (M + \sqrt{M^2+4B_e/3})^2 - B_e$. In what follows, we discuss how to perform an analytic extension of $J^{(B2){\rm ir}}_{\rho^+\rho^+}(0,-m^2)$ in order to get a definite result for the polarization function between these two thresholds. After integration over z, one gets

$$J^{(B2){\rm ir}}_{\rho^+\rho^+}(0,-m^2) = -\frac{N_cB_e}{18\pi^2}\int_{-1}^{1} dv\,\frac{4r_0^2+1-v^2}{(v+\delta)^2+\lambda^2}e^{-(v+\delta)^2-\lambda^2}, \tag{C8}$$

where we have introduced the definitions

$$r_0 = \frac{M}{\sqrt{m^2 + B_e}}, \quad r_d = \sqrt{\frac{M^2 + 2B_e/3}{m^2 + B_e}}, \quad \delta = r_d^2 - r_0^2 \tag{C9}$$

and

$$\lambda^2 = [(r_d + r_0)^2 - 1][1 - (r_d - r_0)^2]. \tag{C10}$$

The expression in Eq. (C8) can be written as

$$\begin{aligned} J^{(B2)\mathrm{ir}}_{\rho^+\rho^+}(0, -m^2) &= \frac{N_c B_e}{18\pi^2} \left\{ \frac{\sqrt{\pi}}{2} e^{-\lambda^2} [\mathrm{erf}(1+\delta) + \mathrm{erf}(1-\delta)] \right. \\ &\quad + \delta[E_1(4r_d^2) - E_1(4r_0^2)] + 2(1 - \delta + \lambda^2) \\ &\quad \left. \times \left[\int_{-1}^{1} dv \frac{1 - e^{-(v+\delta)^2 - \lambda^2}}{(v+\delta)^2 + \lambda^2} + F(m^2 + B_e) \right] \right\}, \end{aligned} \tag{C11}$$

where

$$F(m^2 + B_e) = \int_{-1}^{1} dv \frac{1}{(v+\delta)^2 + \lambda^2}. \tag{C12}$$

For $m < m_{\mathrm{th}}^{(0)}$, one has $\lambda^2 > 0$, and the integral in Eq. (C12) can be done explicitly, leading to

$$F(m^2 + B_e)_{m < m_{\mathrm{th}}^{(0)}} = \frac{1}{\lambda} \left[\arctan\left(\frac{\lambda}{1+\delta} \right) + \arctan\left(\frac{\lambda}{1+\delta} \right) - \pi \right]. \tag{C13}$$

On the other hand, for m beyond the threshold $m_{\mathrm{th}}^{(0)}$, one has $\lambda^2 < 0$. Defining $\bar{\lambda}^2 = -\lambda^2$, the function above can be analytically extended to

$$F(m^2 + B_e)_{m > m_{\mathrm{th}}^{(0)}} = \frac{1}{\bar{\lambda}} \left[\mathrm{arctanh}\left(\frac{\bar{\lambda}}{1+\delta} \right) + \mathrm{arctanh}\left(\frac{\bar{\lambda}}{1+\delta} \right) - i\pi \right], \tag{C14}$$

implying the existence of an absorptive part in the polarization function. At the threshold, one has $r_0 + r_d = 1$; thus, $\lambda^2 = 0$, and $J^{(B2)\mathrm{ir}}_{\rho^+\rho^+}(0, -m^2)$ is divergent.

A similar procedure can be carried out in the case of the magnetic piece of the polarization function $J^{\mathrm{reg}}_{\pi^+\pi^+}(0, -m^2)$, for $m < m_{\mathrm{th}}^{(0)\prime}$. The corresponding expressions are found to be given by

$$J^{\mathrm{mag}}_{\pi^+\pi^+}(0, -m^2) = J^{\mathrm{uv}}_{\pi^+\pi^+}(0, -m^2) + J^{(B1)\mathrm{ir}}_{\pi^+\pi^+}(0, -m^2) + J^{(B2)\mathrm{ir}}_{\pi^+\pi^+}(0, -m^2) + J^{(0)\mathrm{ir}}_{\pi^+\pi^+}(-m^2), \tag{C15}$$

where

$$\begin{aligned} J^{\mathrm{uv}}_{\pi^+\pi^+}(0, -m^2) &= -\frac{N_c}{4\pi^2} \int_{-1}^{1} dv \left\{ \int_0^{4/(m^2+B_e)} dz\, e^{-z[M^2 - (1-v^2)(m^2+B_e)/4]} \right. \\ &\quad \times \left[\frac{(1 - t_u t_d)}{\alpha_+} \left(M^2 + \frac{1}{z} + \frac{1-v^2}{4}(m^2 + B_e) \right) + \frac{(1-t_u^2)(1-t_d^2)}{\alpha_+^2} \right] \\ &\quad \left. - \int_0^{4/m^2} \frac{dz}{z} e^{-z[M^2 - (1-v^2)m^2/4]} \left(M^2 + \frac{2}{z} + \frac{1-v^2}{4} m^2 \right) \right\}, \\ J^{(B1)\mathrm{ir}}_{\pi^+\pi^+}(0, -m^2) &= -\frac{N_c}{4\pi^2} \int_{-1}^{1} dv \int_{4/(m^2+B_e)}^{\infty} dz\, e^{-z[M^2 - (1-v^2)(m^2+B_e)/4]} \\ &\quad \times \left[\left(\frac{(1 - t_u t_d)}{\alpha_+} - \frac{2B_e}{9} e^{-z(1+v)B_e/3} \right) \left(M^2 + \frac{1}{z} + \frac{1-v^2}{4}(m^2 + B_e) \right) + \frac{(1-t_u^2)(1-t_d^2)}{\alpha_+^2} \right], \\ J^{(B2)\mathrm{ir}}_{\pi^+\pi^+}(0, -m^2) &= \frac{N_c B_e}{18\pi^2} \left\{ 2\gamma - 4 + \frac{\sqrt{\pi}}{2} e^{-\lambda^2} [\mathrm{erf}(1+\delta) + \mathrm{erf}(1-\delta)] + 2\ln(4 r_0 r_d) \right. \\ &\quad + \int_{-1+\delta}^{1+\delta} dv \left[2(1 - \delta + \lambda^2) \frac{1 - e^{-(v^2+\lambda^2)}}{v^2 + \lambda^2} - E_{\mathrm{in}}(v^2 + \lambda^2) \right] \\ &\quad \left. + \delta[E_{\mathrm{in}}(4r_d^2) - E_{\mathrm{in}}(4r_0^2)] + 2(1-\delta) F(m^2 + B_e) \right\}, \\ J^{(0)\mathrm{ir}}_{\pi^+\pi^+}(-m^2) &= \frac{N_c m^2}{16\pi^2} \left\{ \int_{-1}^{1} dv (2 + \beta^2 - 3v^2)[-\gamma - \ln|v^2 - \beta^2| + E_{\mathrm{in}}(v^2 - \beta^2)] + 2\sqrt{\pi}\, \mathrm{erf}(1) e^{\beta^2} + i4\pi\beta\theta(\beta^2) \right\}. \end{aligned} \tag{C16}$$

As in the case of the polarization function $J^{\mathrm{reg}}_{\rho^+\rho^+}(0, -m^2)$, for $m > 2M$, the imaginary part in $J^{(0)\mathrm{ir}}_{\pi^+\pi^+}(-m^2)$ cancels with the imaginary part arising from $J^{0,\mathrm{reg}}_{\pi}(-m^2)$, whereas for $m_{\mathrm{th}}^{(0)} < m < m_{\mathrm{th}}^{(0)\prime}$, one gets an absorptive part coming from the function $F(m^2+B_e)$ in $J^{(B2)\mathrm{ir}}_{\pi^+\pi^+}(0,-m^2)$ [beyond $m^{(0)\prime}_{\mathrm{th}}$, another absorptive contribution will arise from $J^{(B1)\mathrm{ir}}_{\pi^+\pi^+}(0,-m^2)$]. Finally, for the mixing polarization function $J_{\rho^+\pi^+}(0,-m^2)$ (which does not need regularization in the ultraviolet limit), we obtain

$$J^{\mathrm{mag}}_{\rho^+\pi^+}(0,-m^2) = J^{\mathrm{uv}}_{\rho^+\pi^+}(0,-m^2) + J^{(B1)\mathrm{ir}}_{\rho^+\pi^+}(0,-m^2) + J^{(B2)\mathrm{ir}}_{\rho^+\pi^+}(0,-m^2), \tag{C17}$$

where

$$\begin{aligned}
J^{\mathrm{uv}}_{\rho^+\pi^+}(0,-m^2) &= \frac{N_c M\sqrt{m^2+B_e}}{4\pi^2}\int_{-1}^{1} dv \int_0^{4/(m^2+B_e)} dz\, \frac{(t_u-t_d)}{\alpha_+}\, e^{-z[M^2-(1-v^2)(m^2+B_e)/4]},\\
J^{(B1)\mathrm{ir}}_{\rho^+\pi^+}(0,-m^2) &= \frac{N_c M\sqrt{m^2+B_e}}{4\pi^2}\int_{-1}^{1} dv \int_{4/(m^2+B_e)}^{\infty} dz\, e^{-z[M^2-(1-v^2)(m^2+B_e)/4]}\left[\frac{t_u-t_d}{\alpha_+} - \frac{2B_e}{9}\, e^{-z(1+v)B_e/3}\right],\\
J^{(B2)\mathrm{ir}}_{\rho^+\pi^+}(0,-m^2) &= -\frac{2N_c M B_e}{9\pi^2\sqrt{m^2+B_e}}\left[\int_{-1+\delta}^{1+\delta} dv\, \frac{1-e^{-(v^2+\lambda^2)}}{v^2+\lambda^2} + F(m^2+B_e)\right],
\end{aligned} \tag{C18}$$

with $F(m^2+B_e)$ given by Eqs. (C12) and (C13).

[1] D. E. Kharzeev, K. Landsteiner, A. Schmitt, and H. U. Yee, Lect. Notes Phys. **871**, 1 (2013).
[2] J. O. Andersen, W. R. Naylor, and A. Tranberg, Rev. Mod. Phys. **88**, 025001 (2016).
[3] V. A. Miransky and I. A. Shovkovy, Phys. Rep. **576**, 1 (2015).
[4] T. Vachaspati, Phys. Lett. B **265**, 258 (1991).
[5] D. Grasso and H. R. Rubinstein, Phys. Rep. **348**, 163 (2001).
[6] R. C. Duncan and C. Thompson, Astrophys. J. Lett. **392**, L9 (1992).
[7] C. Kouveliotou, S. Dieters, T. Strohmayer, J. van Paradijs, G. J. Fishman, C. A. Meegan, K. Hurley, J. Kommers, I. Smith, D. Frail *et al.*, Nature (London) **393**, 235 (1998).
[8] V. Skokov, A. Y. Illarionov, and V. Toneev, Int. J. Mod. Phys. A **24**, 5925 (2009).
[9] V. Voronyuk, V. D. Toneev, W. Cassing, E. L. Bratkovskaya, V. P. Konchakovski, and S. A. Voloshin, Phys. Rev. C **83**, 054911 (2011).
[10] D. E. Kharzeev, L. D. McLerran, and H. J. Warringa, Nucl. Phys. **A803**, 227 (2008).
[11] K. Fukushima, D. E. Kharzeev, and H. J. Warringa, Phys. Rev. D **78**, 074033 (2008).
[12] D. E. Kharzeev, J. Liao, S. A. Voloshin, and G. Wang, Prog. Part. Nucl. Phys. **88**, 1 (2016).
[13] S. P. Klevansky and R. H. Lemmer, Phys. Rev. D **39**, 3478 (1989).
[14] V. P. Gusynin, V. A. Miransky, and I. A. Shovkovy, Nucl. Phys. **B462**, 249 (1996).
[15] G. S. Bali, F. Bruckmann, G. Endrodi, Z. Fodor, S. D. Katz, S. Krieg, A. Schafer, and K. K. Szabo, J. High Energy Phys. 02 (2012) 044.
[16] G. S. Bali, F. Bruckmann, G. Endrodi, Z. Fodor, S. D. Katz, and A. Schafer, Phys. Rev. D **86**, 071502 (2012).
[17] M. N. Chernodub, Phys. Rev. D **82**, 085011 (2010).
[18] M. N. Chernodub, Phys. Rev. Lett. **106**, 142003 (2011).
[19] V. V. Braguta, P. V. Buividovich, M. N. Chernodub, A. Y. Kotov, and M. I. Polikarpov, Phys. Lett. B **718**, 667 (2012).
[20] Y. Hidaka and A. Yamamoto, Phys. Rev. D **87**, 094502 (2013).
[21] C. Li and Q. Wang, Phys. Lett. B **721**, 141 (2013).
[22] H. Liu, L. Yu, and M. Huang, Phys. Rev. D **91**, 014017 (2015).
[23] M. A. Andreichikov, B. O. Kerbikov, E. V. Luschevskaya, Y. A. Simonov, and O. E. Solovjeva, J. High Energy Phys. 05 (2017) 007.
[24] G. S. Bali, B. B. Brandt, G. Endrődi, and B. Gläßle, Phys. Rev. D **97**, 034505 (2018).
[25] G. Cao, Phys. Rev. D **100**, 074024 (2019).
[26] D. N. Voskresensky, Phys. Rev. D **101**, 056011 (2020).
[27] G. Cao, Eur. Phys. J. A **57**, 264 (2021).
[28] S. Fayazbakhsh, S. Sadeghian, and N. Sadooghi, Phys. Rev. D **86**, 085042 (2012).
[29] S. Fayazbakhsh and N. Sadooghi, Phys. Rev. D **88**, 065030 (2013).
[30] S. S. Avancini, W. R. Tavares, and M. B. Pinto, Phys. Rev. D **93**, 014010 (2016).
[31] S. S. Avancini, R. L. S. Farias, M. Benghi Pinto, W. R. Tavares, and V. S. Timóteo, Phys. Lett. B **767**, 247 (2017).
[32] S. Mao and Y. Wang, Phys. Rev. D **96**, 034004 (2017).
[33] R. Zhang, W. j. Fu, and Y. x. Liu, Eur. Phys. J. C **76**, 307 (2016).
[34] D. Gómez Dumm, M. F. Izzo Villafañe, and N. N. Scoccola, Phys. Rev. D **97**, 034025 (2018).
[35] Z. Wang and P. Zhuang, Phys. Rev. D **97**, 034026 (2018).
[36] H. Liu, X. Wang, L. Yu, and M. Huang, Phys. Rev. D **97**, 076008 (2018).

[37] M. Coppola, D. Gómez Dumm, and N. N. Scoccola, Phys. Lett. B **782**, 155 (2018).
[38] S. Mao, Phys. Rev. D **99**, 056005 (2019).
[39] S. S. Avancini, R. L. S. Farias, and W. R. Tavares, Phys. Rev. D **99**, 056009 (2019).
[40] M. Coppola, D. Gomez Dumm, S. Noguera, and N. N. Scoccola, Phys. Rev. D **100**, 054014 (2019).
[41] S. Ghosh, A. Mukherjee, N. Chaudhuri, P. Roy, and S. Sarkar, Phys. Rev. D **101**, 056023 (2020).
[42] S. S. Avancini, M. Coppola, N. N. Scoccola, and J. C. Sodré, Phys. Rev. D **104**, 094040 (2021).
[43] A. Ayala, R. L. S. Farias, S. Hernández-Ortiz, L. A. Hernández, D. M. Paret, and R. Zamora, Phys. Rev. D **98**, 114008 (2018).
[44] K. Kamikado and T. Kanazawa, J. High Energy Phys. 03 (2014) 009.
[45] N. O. Agasian and I. A. Shushpanov, J. High Energy Phys. 10 (2001) 006.
[46] J. O. Andersen, J. High Energy Phys. 10 (2012) 005.
[47] G. Colucci, E. S. Fraga, and A. Sedrakian, Phys. Lett. B **728**, 19 (2014).
[48] M. Kawaguchi and S. Matsuzaki, Phys. Rev. D **93**, 125027 (2016).
[49] V. D. Orlovsky and Y. A. Simonov, J. High Energy Phys. 09 (2013) 136.
[50] C. A. Dominguez, M. Loewe, and C. Villavicencio, Phys. Rev. D **98**, 034015 (2018).
[51] E. V. Luschevskaya, O. A. Kochetkov, O. V. Teryaev, and O. E. Solovjeva, JETP Lett. **101**, 674 (2015).
[52] B. B. Brandt, G. Bali, G. Endrödi, and B. Glässle, *Proc. Sci.*, LATTICE2015 (2016) 265 [arXiv:1510.03899].
[53] E. V. Luschevskaya, O. E. Solovjeva, and O. V. Teryaev, J. High Energy Phys. 09 (2017) 142.
[54] H. T. Ding, S. T. Li, A. Tomiya, X. D. Wang, and Y. Zhang, Phys. Rev. D **104**, 014505 (2021).
[55] U. Vogl and W. Weise, Prog. Part. Nucl. Phys. **27**, 195 (1991).
[56] S. P. Klevansky, Rev. Mod. Phys. **64**, 649 (1992).
[57] T. Hatsuda and T. Kunihiro, Phys. Rep. **247**, 221 (1994).
[58] J. P. Carlomagno, D. Gomez Dumm, S. Noguera, and N. N. Scoccola, Phys. Rev. D **106**, 074002 (2022).
[59] J. S. Schwinger, Phys. Rev. **82**, 664 (1951).
[60] P. G. Allen, A. G. Grunfeld, and N. N. Scoccola, Phys. Rev. D **92**, 074041 (2015).
[61] S. S. Avancini, R. L. S. Farias, N. N. Scoccola, and W. R. Tavares, Phys. Rev. D **99**, 116002 (2019).
[62] D. P. Menezes, M. Benghi Pinto, S. S. Avancini, A. Perez Martinez, and C. Providencia, Phys. Rev. C **79**, 035807 (2009).
[63] V. A. Miransky and I. A. Shovkovy, Phys. Rev. D **66**, 045006 (2002).
[64] A. Ayala, M. Loewe, A. J. Mizher, and R. Zamora, Phys. Rev. D **90**, 036001 (2014).
[65] R. L. S. Farias, K. P. Gomes, G. I. Krein, and M. B. Pinto, Phys. Rev. C **90**, 025203 (2014).
[66] M. Ferreira, P. Costa, O. Lourenço, T. Frederico, and C. Providência, Phys. Rev. D **89**, 116011 (2014).
[67] F. L. Braghin, Phys. Rev. D **94**, 074030 (2016).
[68] G. Endrődi and G. Markó, J. High Energy Phys. 08 (2019) 036.
[69] B. k. Sheng, X. Wang, and L. Yu, Phys. Rev. D **105**, 034003 (2022).
[70] T. H. Moreira and F. L. Braghin, Phys. Rev. D **105**, 114009 (2022).
[71] S. Klimt, M. F. M. Lutz, U. Vogl, and W. Weise, Nucl. Phys. **A516**, 429 (1990).
[72] H. C. Corben and J. Schwinger, Phys. Rev. **58**, 953 (1940).
[73] V. I. Ritus, Sov. Phys. JETP **48**, 788 (1978) [Zh. Eksp. Teor. Fiz. **75**, 1560 (1978)].
[74] A. I. Nikishov, J. Exp. Theor. Phys. **93**, 197 (2001).